GENERIC 2D/3D SMOOTHING VIA REGIONAL VARIATION

Wenfei Jiang, Tao Luo, Fan Zhang, Jiang Tian, Pei Luo, Kangying Cai*

Technicolor

ABSTRACT

In this paper, we propose a method to measure the relationship between data samples, which is dependent on the possibility whether they are within a homogeneous region or not. By considering the regional variation, this possibility is formulated in terms of the maximum local variation along the shortest path connecting the samples. The metric is concretized in both 2D images and 3D meshes, and then integrated into smoothing filters. Benefited from our method, the improved filters tend to effectively preserve the structural component of data. Moreover, our method is implemented in various applications such as image denoising, image decomposition and mesh smoothing, which demonstrates better performance in comparison to the previous work.

Index Terms— Image Smoothing, Mesh Smoothing, Tone Mapping, Adaptive Filter, Image Decomposition

1. INTRODUCTION

Evaluating the relationship among data samples is usually a fundamental step in data restoration and decomposition. An elegant formulation of the sample relationship can be commonly used in image/video editing [1] and 3D processing applications, such as image denoising [2, 3, 4, 5], superpixel [6], tone mapping [7], 3D mesh smoothing [8, 9], etc. An successful example of these works is bilateral filtering [2, 8], in which the spatial closeness and the property similarity contribute to the locally adaptive weights of filtering. In this paper, a generic formulation is proposed to measure the region homogeneity between data samples, and applied to either 2D image or 3D mesh smoothing.

In the prior arts, the regional factors have been considered to improve the performance of previous filters. Nonlocal-means (NLM) filter [3] extends the similarity of pair-wise pixels to that of the neighborhood pairs. One kind of trilateral denoising algorithms [4] estimates the reliability of the filtering neighborhood by impulsive noise detection. Another trilateral filter [10] is fundamentally a piecewise bilateral filter which works in unit of homogeneous region. In [11], the geodesic distances are taken as the filtering weights, which essentially sums up the region-crossing-cost in its path finding process. In this paper, we quantify the region homogeneity (*RH*) into a graded scalar to overcome the uncertainty caused by the thresholding to determine the homogeneous regions in [10]. Moreover, the value of RH takes the maximum of the region-crossing-cost rather than the sum, and thus avoids overestimating the cost across complex texture, which probably occurs in [11].

Take the image in Fig. 1 for example, the region homogeneity between points a and b relies on the local variation (*LV*) along the path $\overline{ab}$. Obviously, the sharp edges between a and b, which correspond to the significant spikes in the white curve, are the key factors determining whether a and b are in a homogeneous region or not. Thus, the region homogeneity between them can be defined as

$$RH_{ab} = \max\{LV_{ij}|i, j \in path_{ab}, j \in N(i)\}, \quad (1)$$

where i and j denote a pair of adjacent data samples. $path_{ab}$ is the predefined shortest path, which can be the geodesic path [11], or the straight line. $N(i)$ denotes the neighborhood of the sample i. For the case of 3D meshes, the path can be defined along the mesh edges or across the mesh triangles. In this paper, the proposed metric of region homogeneity between data samples is concretized in 2D images and 3D meshes respectively. It should be noted that the definition in (1) is not limited to 2D images or 3D meshes, and it can be extended to n-dimensional signals with the corresponding definition of local variation.

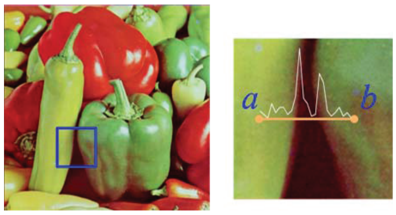

Fig. 1. Region homogeneity and local variation. The white curve denotes the amplitude of *LV* along the orange path.

2. GENERIC REGION HOMOGENEITY FOR 2D IMAGES AND 3D MESHES

As shown in (1), the proposed region homogeneity depends on the definitions of the local variation and the shortest path. In this section, we formulate them for 2D images and 3D meshes, respectively, according to the generic definition.

*Corresponding author: *tao.luo@technicolor.com*

2.1. Formulation in images

The region homogeneity of two pixels in an image I is measured by the maximum local variation along a shortest path between them. Considering that filtering window in most algorithms is relatively small, a straight line between the two pixels is taken as the shortest path in our method. Regarding to the local variation, it is defined on a candidate edge selected in the region surrounded by the two pixels. Intuitively, the possibility of two pixels being in a homogeneous region can be measured by the strongest local variation along the path.

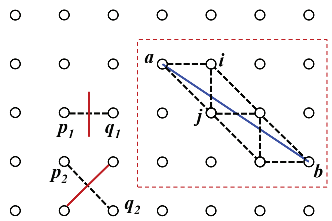

Fig. 2. The *candidate edges* (dashed) along line segment $\overline{ab}$.

As shown in Fig. 2, a part of pixels in the 7×7 window centered at pixel a is depicted and pixel b is one of its neighbors. In order to compute the region homogeneity between pixels a and b, the shortest path is defined as the line segment $\overline{ab}$. And the local variation along $\overline{ab}$ is computed as the strength of a selected candidate edge. In Fig. 2, a dashed edge $\overline{ij}$ indicates a candidate edge, along which the local variation between pixel i and j is defined as,

$$LV_{ij} = |I(i) - I(j)|, \tag{2}$$

where $I(i)$ and $I(j)$ denote the color values of pixel i and pixel j, respectively.

To determine a set of candidate edges Ω_{ab}, the pixels in the region surrounded by a and b are taken into account as the region bounded by the red dash lines in Fig. 2. And the edges connecting a pair of these pixels with the length of 1 or $\sqrt{2}$ are utilized to determine whether they are the candidate edges, which means that only the horizonal, vertical and diagonal edges are considered. For each edge $\overline{ij}$, if its mid-perpendicular segment $\overline{ij}_\perp$ with the length of $\|\overline{ij}\|$ intersects with the line segment $\overline{ab}$, it is selected as the candidate edge to compute local variation. In Fig. 2, the two solid line segments in red are the midperpendicular segments of the edge $\overline{p_1q_1}$ and $\overline{p_2q_2}$, respectively. Thus, the set of candidate edges along $\overline{ab}$ is formulated as,

$$\Omega_{ab} = \{\overline{ij} | \overline{ij}_\perp \cap \overline{ab} \nsubseteq \{\emptyset, a, b\}, \|\overline{ij}_\perp\| = \|\overline{ij}\| = 1 \text{ or } \sqrt{2}\}. \tag{3}$$

Finally, the region homogeneity r_{ab} between a and b is computed by

$$r_{ab} = \max_{\overline{ij} \in \Omega_{ab}} \{LV_{ij}\}. \tag{4}$$

Compared with the geodesic-path based algorithms, less computational expense is cost using our method. Furthermore, the structural feature can be preserved well during filtering operations, which is beneficial for the applications like image denoising or decomposition.

2.2. Formulation in 3D meshes

In this section, we present the region homogeneity between the facets of a 3D mesh, which is defined as the maximum local variation along a shortest path connecting their centroids. The local variation can be measured between two adjacent facets using the geometric attributes, such as position, normal or curvature. And the path is defined on the dual graph of the original mesh using the shortest distance, along which the maximum local variation is obtained.

Given a 3D mesh M with n vertices and m facets, we construct its dual graph G, on which each node represents one facet and each edge indicates the adjacency of two facets. A node of G can be represented by the centroid of its corresponding facet, so there are in total m nodes. To determine the region homogeneity between facet f_a and f_b, where f_b is one of the facets in a predefined neighborhood of f_a, the shortest path $path_{ab}$ between node a and b on the dual graph is approximated using the graph edges with the shortest length. For each constituent edge e_{ij} along the path, the local variation LV_{ij} is computed by $\phi(e_{ij})$. Thus, the region homogeneity r_{ab} can be measured by the maximum local variation along $path_{ab}$, which is expressed as,

$$r_{ab} = \max_{path_{ab}} \{\phi(e_{ij})\}, e_{ij} \in path_{ab}. \tag{5}$$

The local variation $\phi(e_{ij})$ is computed as the difference between the facet variations on node i and j, that is $\phi(e_{ij}) = |\beta_i - \beta_j|$. To calculate the facet variation on each node of the dual graph, we first compute the vertex variation around each vertex on the original mesh. For one vertex v, $N(v)$ denotes the set of its 1-ring neighboring vertices, whose cardinality is $|N(v)|$. Denote by $\mathbf{A}$ the coordinate difference between the neighboring vertices and vertex v, that is $\mathbf{A} = [v_1 - v, \cdots, v_k - v, \cdots, v_{|N(v)|} - v]$. Thus, the covariance matrix around v is computed as,

$$\mathbf{C} = \frac{1}{|N(v)|}\mathbf{A}\mathbf{A}^T. \tag{6}$$

Then, the vertex variation around vertex v can be measured using the three eigenvalues ($\lambda_1 \leq \lambda_2 \leq \lambda_3$) of the matrix $\mathbf{C}$, that is $\alpha_v = \lambda_1/(\lambda_1 + \lambda_2 + \lambda_3)$. For each node of the dual graph, the facet variation β_i is computed as $\beta_i = (\alpha_{v_1} + \alpha_{v_2} + \alpha_{v_3})/3$, where v_1, v_2, v_3 are the vertex indices of the triangular facet f_i.

3. 2D IMAGE AND 3D MESH SMOOTHING

3.1. Image Smoothing

The proposed region homogeneity can be integrated directly into a locally adaptive filtering framework, which is expressed as,

$$h(a) = \frac{\int_{-\infty}^{\infty} f(b)g(\|a-b\|)g(|f(a)-f(b)|)g(r_{ab})\mathrm{d}b}{\int_{-\infty}^{\infty} g(\|a-b\|)g(|f(a)-f(b)|)g(r_{ab})\mathrm{d}b}, \tag{7}$$

where $\|a-b\|$, $|f(a)-f(b)|$ and r_{ab} measure the spatial closeness, the similarity, and the region homogeneity between the target pixel a and a nearby pixel b, respectively. And $g(x)$ denotes a Gaussian function $g(x) = \exp(-x^2/2\sigma^2)$. The influence of the spatial, intensity and region factors are controlled by the corresponding Gaussian parameters σ. Compared to bilateral filter, the computational cost comes from the calculation of four gradient maps for the entire image and the maximization operation for each pixel.

3.1.1. Image Denoising

We apply this filter to image denoising and compare the results with two representative approaches with bilateral (BL) filter [2] and nonlocal-means (NLM) filter [3]. In Fig. 3, the image *womanhat* with Gaussian noise (standard deviation $\sigma = 10$) is denoised by the three approaches. As can be seen, by introducing the factor of the region homogeneity, the result leads to better structure-preserving feature. For Gaussian noise, the performance of our filter is comparable to NLM filter. However, the averaging strategy of NLM filter benefits from the statistics of Gaussian noise rather than other types of noise. As plotted in Fig. 4, our approach has an obvious advantage for Salt&Pepper noise, which demonstrates its robustness to the noise types.

3.1.2. Image Decomposition

The proposed filter (7) is also capable of decomposing an image into a base layer and detail layers as shown in Fig. 5. Image decomposition is employed in various applications such as High Dynamic Range (HDR) imaging. In order to display HDR images on low dynamic range devices, the original set of colors are mapped to a subset [10]. This process, known as tone mapping, decomposes the image and magnifies the detail layers to keep low-contrast details visible. Thus, it is desired that the filter keep the structures of images in the base layer as well as possible.

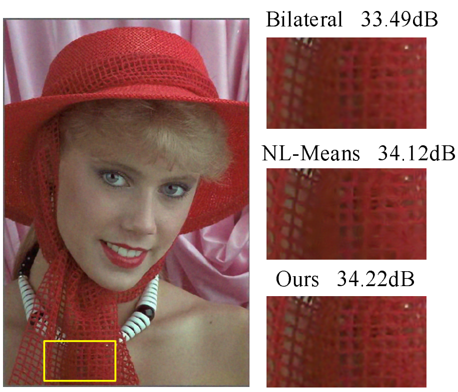

Fig. 3. Subjective quality of the denoised images *womanhat*.

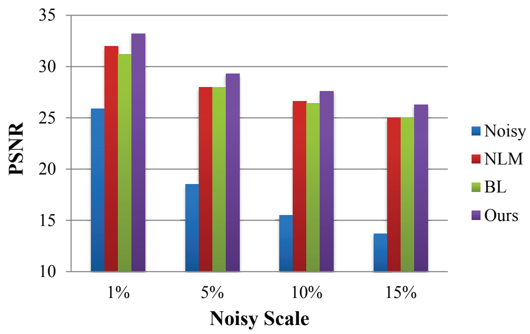

Fig. 4. Denoising results on *House* with Salt&Pepper noise.

Fig. 5. Image decomposition.

Fig. 6 presents the result of tone mapping using the proposed filter. And it can be seen that the detail layer extracted by our approach focuses on the low-contrast textures. In comparison, some structures are involved in the detail layer using bilateral decomposition [7], which makes the detail magnification easily exceed the dynamic range of the devices. Moreover, the edges are usually blurred by bilateral filtering. The blur of the detail layer is magnified by rescaling and therefore some halo-like artifact is then generated. As shown in Fig. 7, tone mapping with bilateral filter generates undesired halo-like artifact along all the edges of the image while our approach produces a more natural appearance.

3.2. Mesh Smoothing

Conventional mesh smoothing methods typically utilize the geometric property (e.g., normal) and the Euclidean distance to measure the correlation between primitives (vertices or facets). In this section, we employ the regional variation to enhance the structure-preserving performance of mesh smoothing. The face normals are first smoothed with consideration of the proposed region homogeneity. Then the vertex coordinates are optimized according to the smoothed normals. This process can be implemented in an iterative manner when the noise is heavy.

To smooth the normal $\mathbf{n}_a$ of a facet f_a, the region homogeneity r_{ab} between facet f_a and its neighboring facet f_b is computed using the aforementioned definition in section 2.2, which allows to enlarge the neighborhood for the smoothing robustness. Since the similarity measurement in bilateral

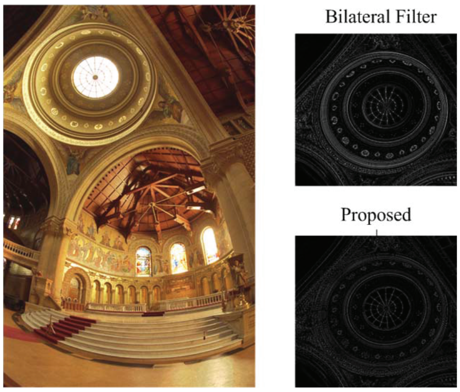

Fig. 6. Tone mapping based on detail magnification.

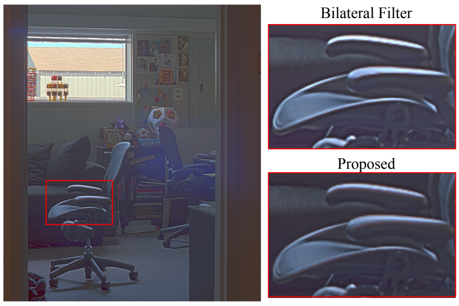

Fig. 7. HDR imaging with bilateral filter and our filter. Our method does not generate undesirable halo artifact.

mesh denoising [8] tends to be unreliable for distant vertices, it is thus replaced by the region homogeneity measurement.

Then, the normal $\mathbf{n}_a$ of facet f_a is smoothed into,

$$\mathbf{n}'_a = \frac{\sum\limits_{f_b \in N(f_a)} g(r_{ab}) g(\|\mathbf{c}_a - \mathbf{c}_b\|) n_b}{\sum\limits_{f_b \in N(f_a)} g(r_{ab}) g(\|\mathbf{c}_a - \mathbf{c}_b\|)}, \tag{8}$$

where $\mathbf{n}_b$ is the normal of facet f_b. And $\mathbf{c}_a$, $\mathbf{c}_b$ denote the centroid positions of f_a, f_b, respectively.

After the face normals are smoothed on the dual graph, the vertex positions can be updated on the original mesh by,

$$\mathbf{v}'_k = \mathbf{v}_k + \frac{1}{|N_f(\mathbf{v}_k)|} \sum_{f_a \in N_f(\mathbf{v}_k)} \mathbf{n}'_a(\mathbf{n}'_a \cdot (\mathbf{c}_a - \mathbf{v}_k)), \tag{9}$$

where $|N_f(\mathbf{v}_k)|$ denotes the number of the neighboring facets of vertex $\mathbf{v}_k$.

In the experiment, the classical bilateral (BL) denoising [8] and the feature-preserving mesh denoising (FPMD) [9] are implemented for comparison. As shown in Fig. 8, the noisy $Igea$ model (courtesy of Cyberware) is smoothed using these three methods. It can be seen that there are more structures using our approach in Fig. 8(d). For quantitative comparison, we employ the $MESH$ tool [12] to compute the mean distance between the smoothed model surfaces and the ground truth. The $Happy\ Buddha$, $Dragon$ (courtesy of Stanford) and $Max\ Planck$ (courtesy of Max Planck Institute) models are artificially corrupted by Gaussian noise with zero mean and variance of $1/5$ of their average edge lengths. As shown in Fig. 9, the offsets of the surfaces smoothed by our method is the smallest among the three methods. Therefore, taking the proposed region homogeneity into consideration is beneficial to mesh denoising while preserving the structures.

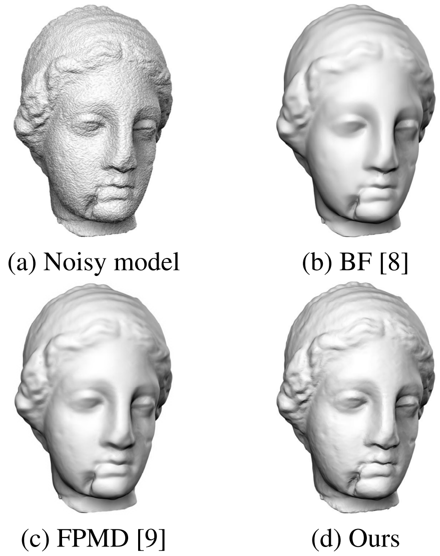

Fig. 8. Comparative results of mesh denoising.

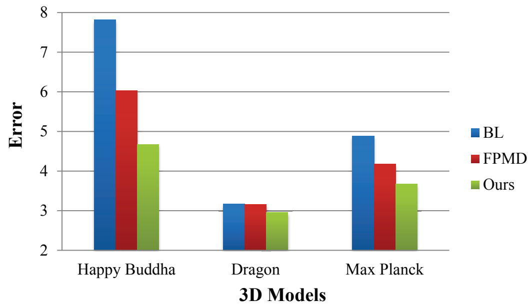

Fig. 9. Error comparison ($\times 10^{-4}$).

4. CONCLUSION

In this paper, we introduce a type of region homogeneity to measure how likely two data samples are within a homogeneous region. Generally, it depends on the maximum local variation along the shortest path connecting data samples for either 2D images or 3D meshes. By considering such a factor in locally adaptive filtering, the structural part of data can be well preserved . As shown in the results of image and mesh smoothing, the improved filters perform better compared with the representative methods. However, the improvement would be limited during image filtering with large window size.

5. REFERENCES

[1] A. Criminisi, T. Sharp, C. Rother, and P. Patrick, "Geodesic image and video editing," *ACM Trans. Graph.*, vol. 29, no. 5, pp. 134:1–134:15, 2010.

[2] C. Tomasi and R. Manduchi, "Bilateral filtering for gray and color images," in *Proc. of ICCV*, 1998, pp. 839–846.

[3] A. Buades, B. Coll, and J. Morel, "A non -local algorithm for image denoising," in *Proc. of CVPR*, 2005, pp. 60–65.

[4] R. Garnett, T. Huegerich, C. Chui, and W.-J. He, "A universal noise removal algorithm with an impulse detector," *IEEE Trans. Image Process.*, vol. 30, no. 6, pp. 1747–1754, 2005.

[5] L. Zhang, W. Dong, D. Zhang, and G. Shi, "Two-stage image denoising by principal component analysis with local pixel grouping," *Pattern Recognition*, vol. 43, no. 4, pp. 1531–1549, 2010.

[6] G. Zeng, P. Wang, J. Wang, R. Gan, and H. Zha, "Structure-sensitive superpixels via geodesic distance," in *Proc. of ICCV*, 2011, pp. 447–454.

[7] S. Paris and F. Durand, "A fast approximation of the bilateral filter using a signal processing approach," in *Proc. of ECCV*, 2006, pp. 568–580.

[8] S. Fleishman, I. Drori, and D. Cohen-Or, "Bilateral mesh denoising," *ACM Trans. Graph.*, vol. 22, no. 3, pp. 950–953, 2003.

[9] X. Sun, P. L. Rosin, R. R. Martin, and F. C. Langbein, "Fast and effective feature-preserving mesh denoising," *IEEE TVCG*, vol. 13, no. 5, pp. 925–938, 2007.

[10] P. Choudhury and J. Tumblin, "The trilateral filter for high contrast images and meshes," in *Proc. of the Eurographics Symp. on Rendering*, 2003, pp. 186–296.

[11] L. Bertelli and B.S. Manjunath, "Edge preserving filters using geodesic distances on weighted orthogonal domains," in *Proc. of ICIP*, Sep. 2007, pp. 321–324.

[12] N. Aspert, D. Santa-Cruz, and T. Ebrahimi, "Mesh: Measuring errors between surfaces using the hausdorff distance," in *Proc. of ICME*, Aug. 2002, pp. 705–708.